Monthly Notices
of the
ROYAL ASTRONOMICAL SOCIETY

MNRAS **490,** 709–717 (2019)
Advance Access publication 2019 September 17

doi:10.1093/mnras/stz2583

Thermal desorption induced by chemical reaction on dust surface

Tetsuo Yamamoto,[1]★ Hitoshi Miura[2] and Osama M. Shalabiea[3,4]

[1]*Institute of Low Temperature Science, Hokkaido University, Sapporo 060-0819, Japan*
[2]*Graduate School of Natural Sciences, Nagoya City University, Nagoya 467-8501, Japan*
[3]*Astronomy, Space Science and Meteorology Department, Faculty of Science, Cairo University, Cairo 12613, Egypt*
[4]*Faculty of Navigation Science and Space Technology (NSST), Beni-Suef University, Beni-Suef, Egypt*

Accepted 2019 September 9. Received 2019 August 6; in original form 2019 April 9

ABSTRACT

We propose a new mechanism of desorption of molecules from dust surface heated by exothermic reactions and derive a formula for the desorption probability. This theory includes no parameter that is physically ambiguous. It can predict the desorption probabilities not only for one-product reactions but also for multiproduct reactions. Furthermore, it can predict desorption probability of a pre-adsorbed molecule induced by a reaction at a nearby site. This characteristic will be helpful to verify the theory by the experiments which involve complex reaction networks. We develop a quantitative method of comparing the predicted desorption probability with the experiments. This method is also applied to the theories proposed so far. It is shown that each of them reproduces the experiments with similar precision, although the amount of systematic experimental data that give definite desorption probability are limited at present. We point out the importance of clarifying the nature of the substrate used in the experiment, in particular, its thermal diffusivity. We show a way to estimate the substrate properties from systematic desorption experiments without their direct measurements.

Key words: astrochemistry – molecular processes – ISM: molecules.

1 INTRODUCTION

The interstellar medium (ISM) out of which stars and planets form has substantial molecular and dust components, which play a fundamental role in the thermal state and evolution of the ISM (see van Dishoeck & Blake 1998; Tielens 2013; Cuppen et al. 2017; van Dishoeck 2017; Yamamoto 2017, and references therein). The observations have revealed the existence of various molecular species including complex organic molecules (COMs) and terrestrial-type organic species in molecular clouds, cold dense cores, and pre-stellar cores, where the temperatures are as low as 10 K (Vasyunin & Herbst 2013). The presence of gaseous molecules in such dense and cold environments indicates that there must be some process that desorbs molecules from dust surface because gaseous molecules accrete on to dust surface within a time shorter than the cloud lifetime and would have been lost from the gas, unless their sticking probability is much less than unity. This is known as the freeze-out paradox (e.g. Williams 1993). Various desorption mechanisms have been proposed for dense and cold clouds such cosmic ray-induced explosive desorption and desorption by grain–grain collisions (Hasegawa & Herbst 1993; Shalabiea & Greenberg 1994; Shen et al. 2004), and impulsive heating by cosmic ray and X-ray (Lèger, Jura & Omont 1985; Ivlev et al. 2015). One of the desorption mechanisms that may work in dense and cold molecular clouds is reactive (or chemical) desorption (Roberts et al. 2007). Reactive desorption was originally proposed by Duley & Williams (1993). They proposed CO desorption associated with H_2 formation on dust surface in the clouds as a mechanism of suppression of the CO freeze-out.

We focus on reactive desorption in this paper. Two theories have been proposed that enable us to evaluate the desorption probability. Garrod, Wakelam & Herbst (2007) applied the Rice–Ramsperger–Kessel (RRK) theory to desorption of a molecule from dust surface. They modified the RRK theory by adding another oscillator representing the molecule–surface bond. Within the framework of the RRK theory, bond energies of adjacent two atoms in a molecule and molecule–surface bond are equal. They assumed both energies are on the order of strength of a van der Waals bond. They introduced an arbitrary parameter measuring the efficiency of transfer of energy released by an exothermic reaction to dust surface. Under these settings, they proposed a formula of the desorption probability of a molecule formed by exothermic reactions on the dust surface. Recently, Minissale et al. (2016) proposed another theory based on kinetic consideration. They assumed that the energy released by an exothermic reaction is quickly thermalized in a newly formed molecule resulting in equipartition of energy to all degrees of freedom of motion of the molecule. Motion of the molecule vertical to the surface leads to a collision with a substrate atom and a resulting rebound of the molecule. They assumed an elastic

★ E-mail: tyamamoto@pop.lowtem.hokudai.ac.jp

collision of the molecule with the substrate atom of some 'effective mass' and derived the desorption probability, which depends on the desorption energy and 'temperature' of the thermalized state. They compared their formula with their experiment for oxidized graphite (HOPG) substrate. Here, the effective mass of 130 amu is adopted for HOPG as a fixed parameter referring to Hayes, Oh & Kondo (2007). Vasyunin et al. (2017) utilized the treatment of reactive desorption based on the experimental results of Minissale et al. (2016). See Cazaux et al. (2016) for astronomical implications of their desorption theory.

In these two theories, transfer of the heat of reaction to the substrate suppresses desorption. However, even if most of the heat escapes to the substrate, it leads to elevation of the substrate temperature and promotes thermal desorption. We explore this possibility and derive a formula of desorption probability based on this view. The desorption probability by this mechanism is determined by the degree of the temperature elevation at and near the reaction site and the cooling rate of the substrate. In other words, the desorption probability reflects the properties of substrates such as their heat capacity and thermal conductivity. In this paper, we propose a theory that takes into account the properties of both molecules and substrate.

The rest of this paper is organized as follows. In Section 2, we present the theory and derive a formula of the desorption probability. A method to compare the theoretical and experimental desorption probabilities is presented in Section 3. Comparison of the theory with the experimental results is given in Section 4. We compare and discuss the previous theories and ours in Section 5. In Section 6, we examine the substrate properties derived from the analysis of the experiments using HOPG substrate and suggest a way to estimate substrate properties from desorption experiments. We discuss desorption of a pre-adsorbed molecule induced by a reaction at the nearby sites in Section 7. Concluding remarks are given in Section 8.

2 THEORY

Fig. 1 shows schematic representation of this theory, which involves the following three processes. (a) Molecules migrate on the dust surface. (b) When two molecules meet at a site on the surface, they react to form a new molecule at a certain probability. In addition, reactions can also occur when a molecule in the gas collides directly with a molecule adsorbed on the dust surface. If the reaction is exothermic, the reaction induces sudden release of energy at the site of molecule formation. (c) After the energy is released, a part of that energy, Q, is transferred to the substrate through vibrational coupling between the formed molecule and the lattice atoms of the substrate.

We model the processes described above as an instantaneous spot heating at the reaction site followed by subsequent cooling due to heat conduction into the substrate. Namely, we assume that the energy Q is transferred to the substrate immediately for simplicity. Resulting temperature elevation leads to desorption of molecules from the reaction site and the ambient sites on the substrate at certain probability during the cooling of the reaction site through heat conduction into the substrate. A part of the heat of reaction might be used as vibrational excitation of a formed molecule if the energy enough to excite the molecule is given to it. In what follows, we ignore the vibrational excitation and assume that the energy transferred to the substrate, Q, is set to equal heat of reaction for clarity of the model.

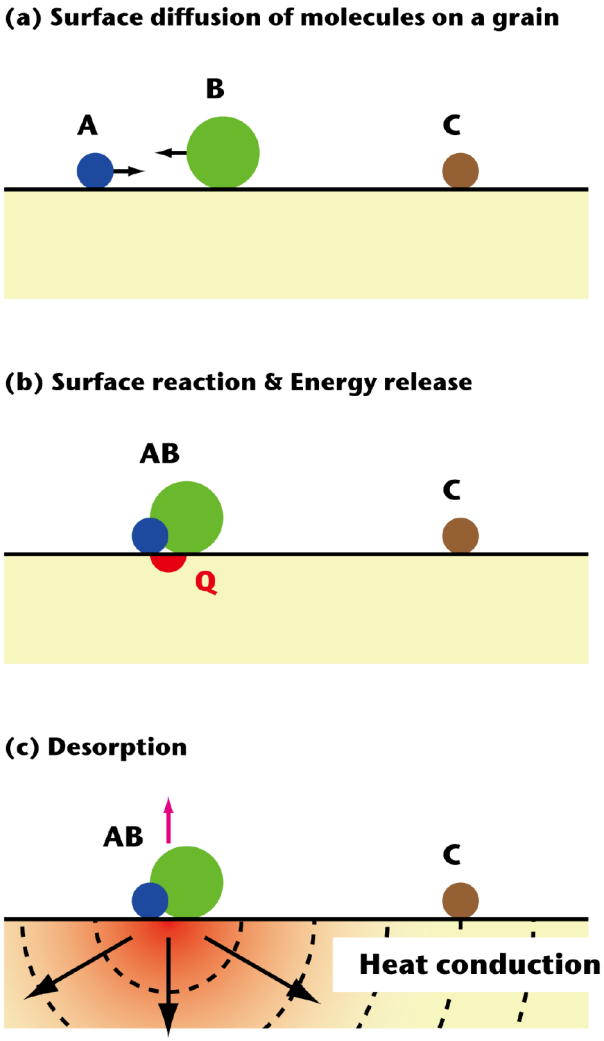

Figure 1. Illustration of our model.

For the temperature $T(t, r)$ at time t at distance r from the reaction site, we adopt the solution of the equation of heat conduction for an instantaneous point source placed in a infinite medium of constant specific heat (e.g. Landau & Lifschitz 1959). In the present situation, however, the medium is semi-infinite and the source is placed on the surface of the medium. As a result, the amount of energy transferred to the medium is twice compared with the case of an infinite medium. The temperature is then given by

$$T(t, r) = \frac{Q}{4\rho c_{\rm p}(\pi\chi t)^{3/2}} {\rm e}^{-r^2/4\chi t} \tag{1}$$

for the substrate of thermal diffusivity χ, mass density ρ, and specific heat $c_{\rm p}$. Here, we assumed $\rho c_{\rm p}$, and χ are constant in deriving equation (1) since desorption occurs at temperatures higher than the Debye temperature in general. At a given distance $r > 0$ from the reaction site, $T(t, r)$ attains a maximum given by

$$T_{\rm m}(r) = \frac{1}{4}\left(\frac{6}{\pi {\rm e}}\right)^{3/2} \frac{Q}{\rho c_{\rm p} r^3} \tag{2}$$

at time

$$t_{\rm m}(r) = \frac{r^2}{6\chi}. \tag{3}$$

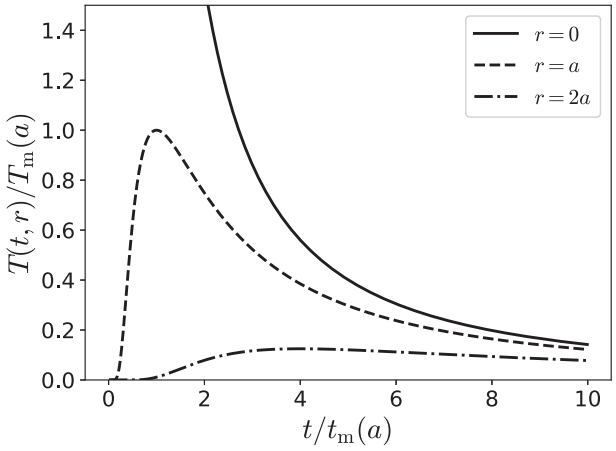

Figure 2. Time variation of the temperature $T(t,\ r)$ at distance $r = 0$, a, and $2a$ from the reaction site of a molecule, where a is size of the sites. Here, the temperature T is scaled by $T_{\rm m}(a)$ given by equation (2), and the time t by $t_{\rm m}(a)$ given by equation (3).

With increasing the distance r from the reaction site, the time of the maximum temperature is delayed in proportion to r^2 and the maximum temperature $T_{\rm m}(r)$ decreases as $1/r^3$. By scaling t by $t_{\rm m}(a)$ and T by $T_{\rm m}(a)$, equation (1) is expressed simply as

$$\frac{T(t,r)}{T_{\rm m}(a)} = \left(\frac{1}{\tau}\right)^{3/2} \exp\left[\frac{3}{2}\left(1-\frac{1}{\tau}\right)\right], \tag{4}$$

where a is size of the site (lattice constant) and

$$\tau = \frac{6\chi t}{r^2}. \tag{5}$$

Fig. 2 shows time variation of the temperature at $r/a = 0,\ 1$ and 2, indicating that the highest temperature is attained at the reaction site $r = 0$ at any time. The time variation of the temperature at $r = 0$ is given by

$$\frac{T(t,0)}{T_{\rm m}(a)} = \left(\frac{{\rm e}\, t_{\rm m}(a)}{t}\right)^{3/2} \tag{6}$$

from equations (1)–(3).

The desorption rate of a molecule adsorbed on the surface of temperature T is expressed by a first-order Polanyi–Wigner equation (e.g. Tielens & Allamandola 1987; King 2007; Miura et al. 2017)

$$p = \nu {\rm e}^{-E_{\rm d}/kT}, \tag{7}$$

where ν is frequency of vibration of an adsorbed molecule vertical to the surface, k is the Boltzmann constant, and $E_{\rm d}$ is activation energy for desorption, which we call desorption energy hereafter. The frequency ν is given (Tielens & Allamandola 1987) by

$$\nu = \sqrt{\frac{2n_{\rm s}E_{\rm d}}{\pi^2\mu m_{\rm a}}}, \tag{8}$$

for a harmonic adsorption potential, where μ is molecular weight of a desorbing molecule, $m_{\rm a} = 1.66 \times 10^{-24}$ g is atomic mass unit, and $n_{\rm s}$ is surface density of the adsorption sites. The surface density is approximated to be $n_{\rm s} \simeq 1/a^2$. Integrating the desorption rate given by equation (7) over time t, the desorption probability of a molecule placed at distance r from the reaction site is expressed by

$$P(r) = \nu \int_0^\infty {\rm d}t\ \exp\left(-\frac{E_{\rm d}}{kT(t,r)}\right). \tag{9}$$

We discuss the desorption probability $P(0)$ at the reaction site $r = 0$ here since the major desorption site is around $r = 0$. The probability of desorption from sites other than $r = 0$ will be discussed in Section 7. $P(0)$ is calculated to be

$$P(0) = 0.114\frac{\nu}{\chi}\left(\frac{kQ}{\rho c_{\rm p}E_{\rm d}}\right)^{2/3}, \tag{10}$$

by substituting $T(t,\ 0)$ given from equation (1), where the numerical coefficient results from $\Gamma(2/3)/(3 \times 2^{1/3}\pi)$ with Γ being the Γ function. It should be pointed out that the $P(0)$ is relatively insensitive to desorption energy, i.e. $P(0) \propto E_{\rm d}^{-1/6}$ as is seen from equations (10) and (8). The probability of desorption during the cooling from T to $T - {\rm d}T$ is proportional to

$$\frac{{\rm e}^{-E_{\rm d}/kT}}{-{\rm d}T/{\rm d}t}{\rm d}T \propto \frac{{\rm e}^{-E_{\rm d}/kT}}{T^{5/3}}{\rm d}T \tag{11}$$

at the reaction site ($r = 0$). Thus, maximum desorption occurs at the temperature of $3E_{\rm d}/5k$. Note that desorption at the initial cooling stage around $t = 0$ is negligible in spite of high temperatures because the cooling rate $-{\rm d}T/{\rm d}t \propto T^{5/3}$ is extremely high.

3 METHOD OF COMPARISON WITH EXPERIMENTS

For comparison with experiments, we use the desorption probability $P(0)$ given by equation (10) as a first approximation. The $P(0)$ includes the substrate properties such as χ and $\rho c_{\rm p}$, which are not known for the substrates used in the experiments. To separate the substrate quantities from other ones, we introduce a parameter P_0 defined by

$$P_0 = 0.114\frac{\nu_0}{\chi}\left(\frac{kQ_0}{\rho c_{\rm p}E_{\rm d0}}\right)^{2/3} \tag{12}$$

with

$$\nu_0 = \left(\frac{2n_{\rm s}E_{\rm d0}}{\pi^2 m_{\rm a}}\right)^{1/2}. \tag{13}$$

Q_0 and $E_{\rm d0}$ can be set to arbitrary typical values of Q and $E_{\rm d}$, respectively. With the use of P_0, the desorption probability $P_i(0)$ is expressed by

$$P_i(0) = P_0 f_i, \quad f_i = \frac{(Q_i/Q_0)^{2/3}}{\mu_i^{1/2}(E_{{\rm d}i}/E_{\rm d0})^{1/6}}, \tag{14}$$

where the suffix i is the number assigned to the reaction. We set $Q_0 = 1$ eV and $E_{\rm d0} = 1000\,{\rm K} = 8.6 \times 10^{-2}$ eV. Note that $P_i(0)$ is independent of the choice of the values of Q_0 and $E_{\rm d0}$. Let us define the deviation of the desorption probability of $P(0)$ from the experimentally measured one, $P_{\rm exp}$, by

$$\sigma^2 = \frac{1}{n}\sum_i (P_i(0) - P_{{\rm exp},i})^2 = \frac{1}{n}\sum_i (P_0 f_i - P_{{\rm exp},i})^2. \tag{15}$$

The summation is taken over the reactions to be compared with the experiments (see Section 4 for details). The value of P_0 that minimizes σ^2 is obtained from ${\rm d}\sigma^2/{\rm d}P_0 = 0$ to be

$$P_0 = \frac{\sum_i P_{{\rm exp},i} f_i}{\sum_i f_i^2}. \tag{16}$$

4 COMPARISON WITH EXPERIMENT

Quantitative experimental study in the astrophysical context was initiated by Dulieu et al. (2013). Minissale et al. (2016) carried out

Table 1. Data of the reactions (Cazaux et al. 2016; Minissale et al. 2016) and theoretical desorption probability $P(0)$ for the oxidized HOPG substrate.

	Reaction	Q (eV)	E_d (K)	μ	$P(0)$	P_{exp}	# 1	# 2	# 3
A1	$N + N \rightarrow N_2$	9.79	790	28	0.67–0.92	> 0.70	✓		
A2	$CO + O \rightarrow CO_2$	5.51	2300	44	0.30–0.42	< 0.05	✓	✓	
A3	$OH + H \rightarrow H_2O$	5.17	4800	18	0.40–0.58	0.50 ± 0.25	✓	✓	✓
A4	$OH + H \rightarrow H_2O$	5.17	4800	18	0.40–0.58	$< 0.80 \pm 0.20$	✓		
A5	$O + O \rightarrow O_2$	5.16	1250	32	0.38–0.52	0.8 ± 0.1	✓	✓	✓
A6	$CH_3O + H \rightarrow CH_3OH$	4.56	3700	32	0.29–0.40	< 0.08	✓	✓	
A7	$O + H \rightarrow OH$	4.44	4600	17	0.38–0.52	0.50 ± 0.25	✓	✓	✓
A8	$HCO + H \rightarrow H_2CO$	3.91	3700	30	0.27–0.37	0.10 ± 0.05	✓	✓	✓
A9	$HCO + H \rightarrow H_2CO$	3.91	3700	30	0.27–0.37	< 0.08	✓	✓	
A10	$O_2 + O \rightarrow O_3$	1.1	2100	48	0.10–0.14	< 0.05	✓	✓	
A11	$H_2CO + H \rightarrow CH_3O$	0.88	3700	31	0.099–0.14	< 0.08	✓	✓	
A12	$CO + H \rightarrow HCO$	0.66	1600	29	0.097–0.13	0.10 ± 0.08	✓	✓	✓
A13	$H_2CO + O \rightarrow CO_2 + H_2$	5.45	2300, 300	44, 2	0.30–0.42, 2.0–2.7	< 0.10			
A14	$HCO + H \rightarrow CO + H_2$	3.85	1100, 300	28, 2	0.34–0.47, 1.6–2.1	0.4 ± 0.2			
A15	$O_3 + H \rightarrow O_2 + OH$	3.33	1250, 4600	32, 17	0.28–0.39, 0.31–0.43	< 0.08			
A16	$H_2O_2 + H \rightarrow H_2O + OH$	2.95	4800, 4600	18, 17	0.28–0.38, 0.29–0.40	No data			
A17	$O_2H + H \rightarrow 2OH$	1.47	4600	17	0.36–0.50	No data			
A18	$H_2CO + H \rightarrow HCO + H_2$	0.61	1600, 300	29, 2	0.092–0.13, 0.46–0.64	0.10 ± 0.05			

comprehensive desorption experiment by means of quadrupole mass spectroscopy for various reactions on the three kinds of substrates of oxidized graphite (HOPG), non-porous amorphous water ice (np-ASW) and amorphous silicate. More recently, Chuang et al. (2018) set upper limit for the desorption probability in the hydrogenation reactions of CO to form H_2CO and CH_3OH on ice substrate by means of infrared spectroscopy. Oba et al. (2018) measured desorption probability of H_2S formed by the reactions with H atoms on the amorphous ice substrate by infrared spectroscopy.

In the lack of the data on the properties of the substrate used in the experiments, we need many reactions on the same substrate to constrain the value of P_0. For systematic comparison of the theory with the experiment, we use the data compiled by Minissale et al. (2016), which meet the above requirement. For the desorption energy E_d, they classified the substrates into two kinds, that is, bare and icy substrates, and listed the values of E_d for various molecular species on these two kinds of substrates. We use equation (16) for determining P_0. Here, we adopt the desorption probability P_{exp} measured for one-product reactions given in table 1 of Minissale et al. (2016); the errors of P_{exp} are ignored for simplicity. Using P_0 values thus determined, we calculate $P(0)$ from equation (14) for each reaction i including $P(0)$ for two-product reactions and those of no measurement.

4.1 Oxidized HOPG substrate

Table 1 summarizes theoretical desorption probability $P(0)$ calculated from equation (14) and P_{exp} for the oxidized HOPG substrate together with the relevant quantities (Cazaux et al. 2016; Minissale et al. 2016). Table 1 lists the values of Q, E_d, and μ used in calculating f_i defined by equation (14). The reactions A1–A12 are one product reactions, and A13–A18 are two-product reactions. The reactions are listed according to the descending order of the values of Q. Many of the P_{exp} are upper or lower limits, and there are small number of the data that give definite value of P_{exp}. So we examine three choices of the reactions to calculate P_0 as shown the last three columns in Table 1. Case #1 chooses all one-product reactions from A1 to A12 with treating the upper and lower limits as the definite values, and case #3 chooses the reactions that give definite P_{exp}. Case #2 chooses all one-product reactions except two reactions that

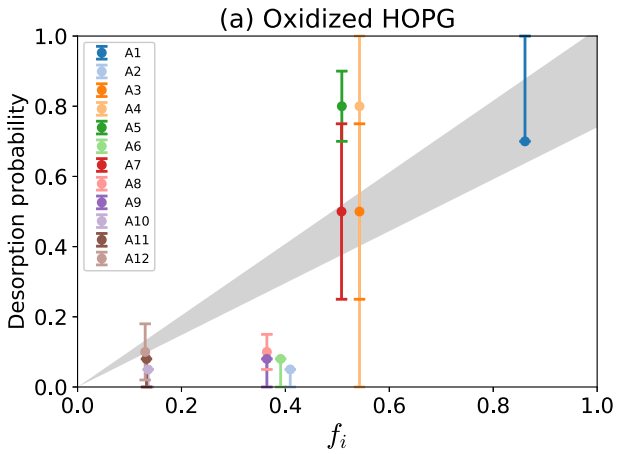

Figure 3. Comparison with the experimental data of one-product reactions for the oxidized HOPG substrate. The values of P_0 are $P_0 = 0.839$ for case #1, $P_0 = 0.745$ for case #2, and $P_0 = 1.02$ for case #3. The range of the theoretical desorption probability $P(0)$ is shown by the gray zone in the figure.

allow large ranges of P_{exp}. The values of P_0 thus calculated are $P_0 = 0.85$ for case #1, $P_0 = 0.74$ for case #2, and $P_0 = 1.02$ for case #3. The values of $P(0)$ given in Table 1 are calculated with the use of equation (14) by using the three possible values of P_0 given above. The deviations are $\sigma = 0.21$, 0.19, and 0.18 for cases #1, #2, and #3, respectively. It is remarkable that the P_0 values for the three cases agree within a factor of 1.4, indicating that the choice of the three cases affects little to the P_0 value, in consequence, the theoretical desorption probability $P(0)$. Fig. 3 shows the results of comparison of the theory and experiments for the one-product reactions on the oxidized HOPG substrate. We showed the range of $P(0)$ bounded by $P_0 = 0.74$ and 1.02 in Fig. 3.

It should be pointed out that this theory can deal with two-product reactions as well if $E_d \ll Q$ as is usually the case. Since two molecules produced by a reaction 'feel' the same substrate temperature, they desorb independently from the substrate surface, but the desorption probability for each of the molecules depends on its E_d and mass. The reactions A13–A18 in Table 1 are two-product

Table 2. Data of the reactions (Cazaux et al. 2016; Minissale et al. 2016) and theoretical desorption probability $P(0)$ for non-porous amorphous water ice (np-ASW) substrate.

	Reaction	Q (eV)	E_d (K)	μ	$P(0)$	P_{exp}	# 1	# 2	# 3
B1	$N + N \rightarrow N_2$	9.79	1140	28	0.27–0.44	> 0.5	✓		
B2	$CO + O \rightarrow CO_2$	5.51	2300	44	0.13–0.21	< 0.05	✓	✓	
B3	$OH + H \rightarrow H_2O$	5.17	4800	18	0.17–0.28	0.30 ± 0.15	✓	✓	✓
B4	$OH + H \rightarrow H_2O$	5.17	4800	18	0.17–0.28	$< 0.4 \pm 0.2$	✓		
B5	$O + O \rightarrow O_2$	5.16	1200	32	0.16–0.27	< 0.05	✓	✓	
B6	$CH_3O + H \rightarrow CH_3OH$	4.56	3700	32	0.13–0.21	< 0.08	✓	✓	
B7	$O + H \rightarrow OH$	4.44	4600	17	0.16–0.27	0.25 ± 0.15	✓	✓	✓
B8	$O_2H + H \rightarrow H_2O_2$	3.69	6000	34	0.097–0.16	< 0.08	✓	✓	
B9	$O_2 + H \rightarrow O_2H$	2.24	4000	33	0.076–0.12	< 0.08	✓	✓	
B10	$O_2 + O \rightarrow O_3$	1.1	2100	48	0.044–0.071	< 0.05	✓	✓	
B11	$H_2CO + O \rightarrow CO_2 + H_2$	5.45	2300, 500	44, 2	0.13–0.21, 0.79–1.3	< 0.1			
B12	$H_2O_2 + H \rightarrow H_2O + OH$	2.95	4800, 4600	18, 17	0.12–0.20, 0.12–0.20	< 0.05			
B13	$O_2H + H \rightarrow 2OH$	1.47	4600	17	0.16–0.26	< 0.08			

reactions. The values of $P(0)$ listed in the table show ranges of the predicted desorption probability for two-product reactions. For the desorption probability for the reaction A17 producing two OH molecules, we set their desorption probability twice the value of $P(0)$ calculated by using equation (14). It is interesting to note high-desorption probability of H_2 molecules in the reactions A13 and A14; $P(0) > 1$ implies that H_2 molecules produced by the reactions have excess energy in desorbing from the adsorption potential well of the substrate. This is due to small mass of H_2 molecules and relatively large Q (i.e. $P(0) \propto Q^{2/3}/\mu^{1/2}$). On the other hand, the desorption probability of H_2 produced by the reaction A18 is lower because of low Q of this reaction.

4.2 Ice substrate

Table 2 compiles the reactions and relevant quantities such as Q, E_d, and μ for np-ASW substrate (Cazaux et al. 2016; Minissale et al. 2016). We take the same procedure as in the case of oxidized HOPG substrate, and examine three choices of the reactions to estimate the value of P_0 as shown in the last three columns in Table 2. We obtained $P_0 = 0.46$ for case #1, $P_0 = 0.32$ for case #2, and $P_0 = 0.52$ for case #3. The values of $P(0)$ given in Table 2 are calculated in the same manner as in the case of the HOPG substrate by using these three possible values of P_0. The deviations are $\sigma = 0.103$, 0.075, and 0.016 for cases #1, #2, and #3, respectively. The range of the P_0 values for the three cases is within in a factor of 1.6, although the σ values for the three cases are scattered. Fig. 4 compares theoretical desorption probability $P(0)$ and the measured ones P_{exp} for the one-product reactions on the np-ASW substrate. The range of $P(0)$ is bounded by $P_0 = 0.32$ and 0.52. Table 2 also shows prediction of the desorption probability $P(0)$ for two-product reactions B11–B13; we set the desorption probability twice the value of $P(0)$ given by equation (14) for the reaction reactions B13 producing two OH molecules. High-desorption probability of H_2 is predicted as was the case of the oxidized HOPG substrate.

4.3 Amorphous silicate substrate

Table 3 shows the reactions and relevant quantities for amorphous silicate substrate (Cazaux et al. 2016; Minissale et al. 2016). The P_0 values obtained for the three choices of the reactions shown in Table 3 are $P_0 = 0.93$ for case #1, $P_0 = 0.95$ for case #2, and $P_0 = 1.09$ for case #3. The range of the $P(0)$ values using these

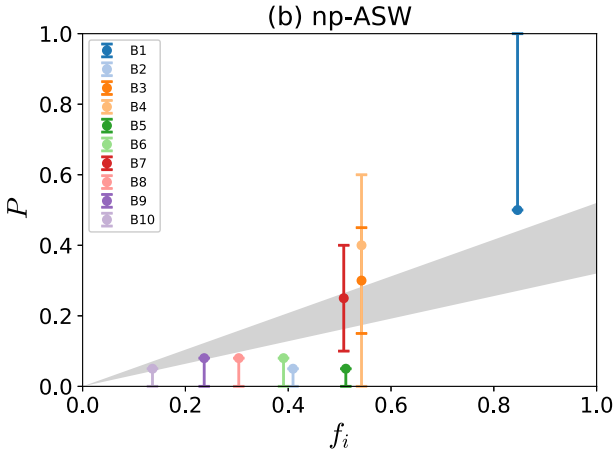

Figure 4. Comparison with the experimental data of one-product reactions for the non-porous amorphous water ice substrate. $P_0 = 0.457$ for case #1, $P_0 = 0.320$ for case #2, and $P_0 = 0.524$ for case #3. The range of the theoretical desorption probability $P(0)$ is shown by the gray zone in the figure.

three P_0 values are given in Table 3. The values of σ are 0.18 for the all cases. The range of the P_0 values for the three cases is the smallest among the three substrates and is within in a factor of 1.2. Fig. 5 compares the desorption probabilities $P(0)$ and P_{exp} for the one-product reactions. The range of $P(0)$ is bounded by $P_0 = 0.93$ and 1.09. Table 3 also lists predicted desorption probability $P(0)$ for two-product reactions C8–C10; we set the desorption probability twice the value of $P(0)$ given by equation (10) for the reaction C10.

5 COMPARISON OF THE THREE THEORIES

Garrod et al. (2007) proposed a formula for the desorption probability by modifying the RRK theory. The RRK theory has been applied to unimolecular reactions in a gas and deals with a spontaneous decomposition of a molecule. In this theory, a molecule is modelled to be an ensemble of oscillators, which represent bonds between atoms in a molecule. It is assumed that the frequencies ν of all oscillators are equal. In other words, bond energy of each pair of atoms in the molecule is assumed to be equal to $h\nu$, where h is Planck's constant. Garrod et al. (2007) added another oscillator representing molecule–surface bond to the original molecule and

Table 3. Data of the reactions (Cazaux et al. 2016; Minissale et al. 2016) and theoretical desorption probability $P(0)$ for the amorphous silicate substrate.

	Reaction	Q (eV)	E_d (K)	μ	$P(0)$	P_{exp}	# 1	# 2	# 3
C1	$N + N \rightarrow N_2$	9.79	790	28	0.84–0.98	> 0.7	✓		
C2	$OH + H \rightarrow H_2O$	5.17	4800	18	0.50–0.59	0.8 ± 0.2	✓	✓	✓
C3	$OH + H \rightarrow H_2O$	5.17	4800	18	0.50–0.59	$< 0.7 \pm 0.2$	✓		
C4	$O + O \rightarrow O_2$	5.16	1250	32	0.47–0.55	0.4 ± 0.1	✓	✓	✓
C5	$O_2H + H \rightarrow H_2O_2$	3.69	6000	34	0.28–0.33	< 0.05	✓	✓	
C6	$O_2 + H \rightarrow O_2H$	2.24	4000	33	0.22–0.27	0.1 ± 0.1	✓	✓	✓
C7	$O_2 + O \rightarrow O_3$	1.1	2100	48	0.13–0.15	< 0.05	✓	✓	
C8	$O_3 + H \rightarrow O_2 + OH$	3.33	1250, 4600	32, 17	0.35–0.41, 0.39–0.46	< 0.25			
C9	$H_2O_2 + H \rightarrow H_2O + OH$	2.95	4800, 4600	18, 17	0.35–0.41, 0.36–0.42	< 0.13			
C10	$O_2H + H \rightarrow 2OH$	1.47	4600	17	0.45–0.53	< 0.05			

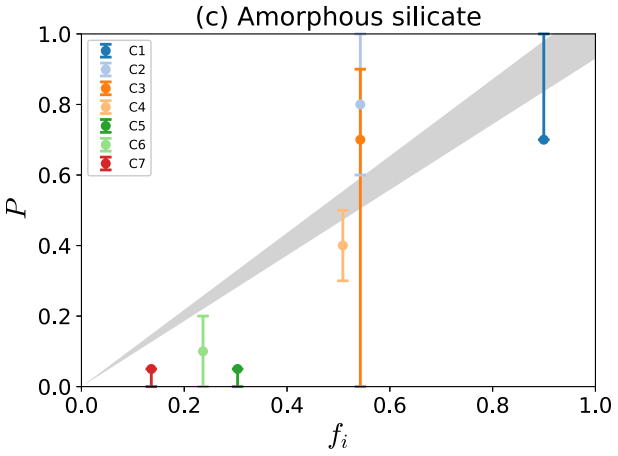

Figure 5. Comparison with the experimental data of one-product reactions for the amorphous silicate substrate. $P_0 = 0.928$ for case #1, 0.949 for case #2, and 1.09 for case #3. The range of the theoretical desorption probability $P(0)$ is shown by the gray zone in the figure.

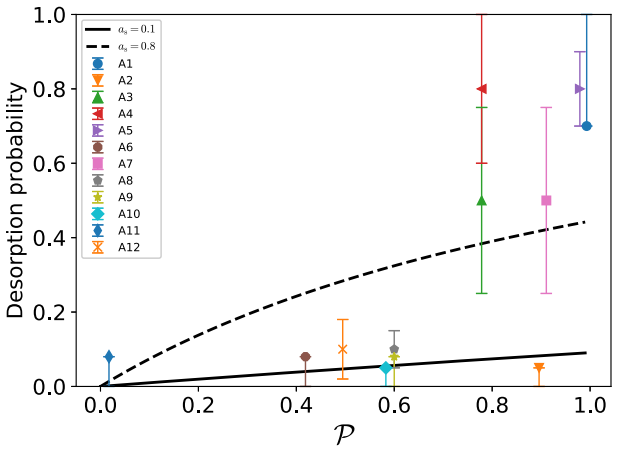

Figure 6. Comparison of the desorption probability P given by equation (17) for the HOPG substrate with those for the reactions A1–A12 in Table 1. The horizontal axis $\mathcal{P}$ is defined by equation (18). The curves show P for $a_s = 0.1$ (solid curve) and $a_s = 0.8$ (dashed curve).

considered a 'compound molecule' including a surface atom. The frequency of the added oscillator must be equal to ν within the framework of the RRK theory. They assumed that $h\nu$ is on the order of the desorption energy E_d. To take energy transfer from the molecules to the surface into account, they introduced a parameter a_s and put $a_s = \nu\tau_s$, where τ_s is a time-scale of the energy transfer to the surface. They expressed the desorption probability by

$$P = \frac{a_s \mathcal{P}}{1 + a_s \mathcal{P}} \tag{17}$$

with

$$\mathcal{P} = (1 - E_d/Q)^{s-1}, \tag{18}$$

where s is the total number of vibration modes of the compound molecule including the molecule–surface bond. Here, $\mathcal{P}$ is the probability of concentration of the vibration energy higher than E_d to a particular bond. Note that the desorption probability P given by equation (17) does not include mass of product molecules. They put $a_s = 0,\ 0.01,\ 0.03$, and 0.1. Fig. 6 compares equation (17) with the desorption probability measured for the reactions A1–A12 in Table 1. The figure shows that $a_s = 0.1$, the largest value of a_s they took, reproduces the experimental results for small $\mathcal{P} \lesssim 0.6$ but not for $\mathcal{P} \gtrsim 0.8$. We found that $a_s = 0.8$ yields minimum deviation of $\sigma = 0.25$, where we set the upper and lower limits of the experimental data to be the definite values for simplicity. We carried out similar analyses for np-AWS and amorphous silicate substrate as well with treating the upper and lower limits as the definite values. The results are $a_s = 0.3$ with $\sigma = 0.14$ for the np-AWS substrate, and $a_s = 1.0$ with $\sigma = 0.28$ for the amorphous silicate substrate. We should note, however, that the results are less reliable compared with those for the HOPG because the experimental data are mostly upper limits. Physically, $a_s = \nu\tau$ is the number of vibrations of a molecule–surface bond during the time-scale of energy transfer to the substrate, so it seems improbable to set $a_s \ll 1$ since the energy must be transferred through this vibration.

Minissale et al. (2016) proposed an alternative theory based on kinetic consideration. They modelled the desorption process into three steps: (1) energy release due to the exothermic reaction to form a molecule, (2) rapid thermalization of this energy among all degrees of freedom of its motion, and (3) the energy imparted to vertical motion of the product molecule leads to desorption at certain probability through a collision with the surface atom (see fig. 4 in their paper). They simplified the step 3. Namely, they assumed that a newly formed molecule makes an elastic collision with the surface atom of certain effective mass and gains velocity in the direction perpendicular to the surface. This is a kinetic process and one can calculate the fraction $\epsilon = (M - m)^2/(M + m)^2$ of kinetic energy given to the product molecule, where m is mass of a product molecule and M is effective mass of the substrate. The step 2 assumes that equipartition of energy to all freedom of motions is realized quickly before the collision. They defined the temperature

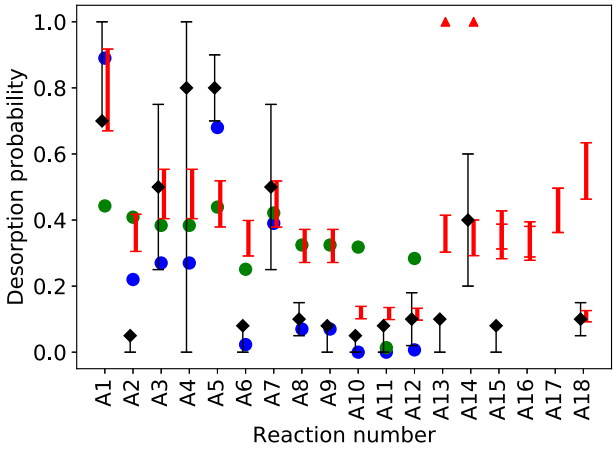

Figure 7. Comparison of the desorption probability predicted by the three theories for oxidized HOPG substrate. The numbers in the horizontal axis correspond to the reaction numbers given in Table 1. Red symbols show the desorption probability $P(0)$ given by this theory including the two-product reactions A13–A18. The bars indicate the ranges of $P(0)$ when taking the P_0 values for the cases #1 to #3. For H_2 produced by the reactions A13 and A14 indicated by the red triangles, we set $P(0) = 1$ (see Section 4.1). Blue dots indicate desorption probability given by Minissale et al. (2016), and green dots by Garrod et al. (2007) for $a_s = 0.8$. Black diamonds with error bars show measured desorption probability given in Table 1. For two-product reactions, there are no data of the desorption probabilities for the reactions A16 and A17.

by $T = \epsilon Q/kN$ under the assumption of the equipartition of energy, where N is the degree of freedom of motion of a desorbing molecule. Under these settings, they gave the desorption probability expressed by

$$P = \exp\left(-\frac{E_d}{kT}\right) = \exp\left[-\frac{NE_d}{Q}\left(\frac{M+m}{M-m}\right)^2\right]. \quad (19)$$

Here, P is the probability of the molecule to have energy higher than the desorption energy E_d, namely, its desorption probability.

In the limiting case of complete energy loss to the substrate, no desorption occurs according to the theories of Garrod et al. (2007) ($a_s = 0$) and Minissale et al. (2016) ($M = m$). In contrast, the desorption probability becomes maximum in this theory (see equation 10). The opposite effect of energy transfer to the substrate on the desorption is a remarkable difference between the previous and present theories.

Fig. 7 compares desorption probability predicted by the three theories with the experiments for oxidized HOPG substrate. Desorption probability predicted by this theory for the two-product reactions is also included for both of the desorbed molecules. Using the data for one-product reactions, we calculated the deviations σ^2 for which $P_i(0)$ in equation (15) is replaced by the values predicted by the formulae of Minissale et al. (2016) and Garrod et al. (2007). The result is $\sigma = 0.19$ for Minissale et al. (2016) for their adopted effective mass of 130 amu for a carbon ring of graphite in oxidized HOPG substrate, and $\sigma = 0.25$ for Garrod et al. (2007) with $a_s = 0.8$. Both σ are close to our $0.18 \leq \sigma \leq 0.21$ (see Section 4.1). It is remarkable that the three theories give comparable values of σ. This indicates that only the comparison with the present experiments does not discriminate the theories. This is not only due to the lack of the sufficient data yielding definite values of the desorption probability but also due to insufficient characterization of the nature of the substrates used in the experiments.

Minissale et al. (2016) pointed out that a comparison of the desorption probabilities of O_2 formed via the reaction A5, B5, C4 with those of O_3 formed via the reaction A10, B10, C9 in Tables 1–3 can be a benchmark test of the theories because of their unambiguous formation routes in the experiment. Their experiment showed that (1) the desorption probability of O_2 is higher than that of O_3 for the three kinds of substrates that they used, and (2) the desorption probability of O_2 is the highest for HOPG substrate and the lowest for np-ASW substrate (see table 1 of Minissale et al. 2016). They claimed that the formula of Garrod et al. (2007) given by equation (17) yields desorption probabilities nearly equal to $a_s/(1 + a_s)$ for both reactions of A5, B5, C4 and A10, B10, C9 since $E_d/Q \ll 1$, thus yields almost the same desorption probability for O_2 and O_3. On the other hand, the formula of Minissale et al. (2016) given by equation (19) explains the higher desorption efficiency of O_2 than O_3 as observed in their experiment according to our theory. Our formula given by equation (10) also reproduces the tendencies (1) and (2) of the experimental results stated above (see Tables 1–3). The desorption probability of O_2 higher than that of O_3 is mainly due to heat of reaction of O_2 larger than O_3.

6 EXAMINATION OF THE VALUE OF P_0

The desorption probability $P(0)$ given by equation (10) includes explicitly the substrate properties such as thermal diffusivity χ and heat capacity ρc_p per unit volume of the substrate. Since the substrate properties used in the experiments were not known well, we introduced the parameter P_0 given by equation (12) and determined its value from minimization of σ defined by equation (15). We shall examine whether the P_0 values thus determined are physically reasonable ones by estimating it from the properties of the substrate.

Since thermal diffusivity is expressed as $\chi = c_s l/3$ in terms of sound speed c_s and mean free path of photons l in the substrate (e.g. Kittel 1986), P_0 is expressed by

$$P_0 = \frac{0.34}{\pi c_s}\left(\frac{2E_{d0}}{m_a}\right)^{1/2}\left(\frac{k}{\rho c_p a^3}\right)^{2/3}\left(\frac{Q_0}{E_{d0}}\right)^{2/3}\frac{a}{l}$$

$$= 2.8\left(\frac{c_s}{\mathrm{km\,s^{-1}}}\right)^{-1}\left(\frac{\rho c_p a^3}{10^{-16}\,\mathrm{erg\,K^{-1}}}\right)^{-2/3}\frac{a}{l}, \quad (20)$$

where we set $n_s = 1/a^2$.

Let us estimate the value of P_0 by taking graphite as an analogue of the oxidized HOPG substrate, for example. We adopt $\rho = 2.2\,\mathrm{g\,cm^{-3}}$ (Zhernokletov et al. 2007) and $c_p = 0.71 \times 10^7\,\mathrm{erg\,g^{-1}\,K^{-1}}$ (Chronological Sciientific Tables 2010). We take $a = 2.5$ Å, which is the length of the a-axis of graphite. Sound speed c_s in graphite depends on the type of graphite and the modes of sound, and is within the range of $1.35 \leq c_s \leq 3.29\,\mathrm{km\,s^{-1}}$ (Zhernokletov et al. 2007). We adopt here a representative value of $c_s = 2\,\mathrm{km\,s^{-1}}$. These values lead to $P_0 = 0.76(a/l)$. On the other hand, P_0 estimated from minimization of σ is $0.75 \leq P_0 \leq 1.0$, which is close to the P_0 for $l \sim a$. It is unfortunately difficult to examine the values of P_0 for the ice and silicate substrates used in the experiments because of their little characterization. However, $(l/a)P_0$ is estimated to be on the order of 0.1–1 from equation (20) since the sound speed c_s is a few times $\mathrm{km\,s^{-1}}$ and the heat capacity per site is around k to $10k$ at temperatures of active desorption for many solids. The quantity of the largest uncertainty is the phonon mean free path l, in other words, thermal diffusivity χ, which depends on the microscopic structure of the substrate such

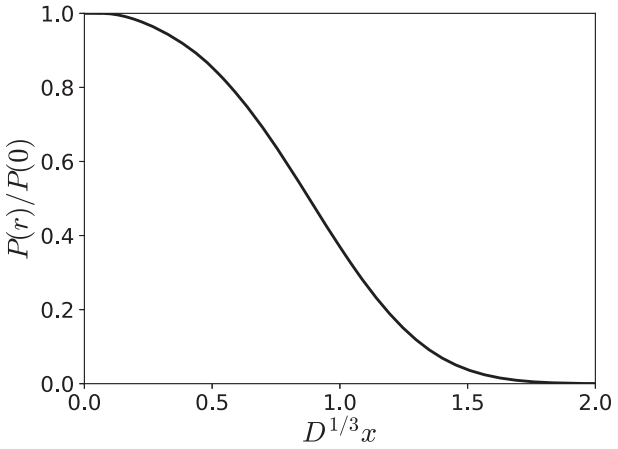

Figure 8. Ratio of the desorption probabilities $P(x)/P(0)$ as a function of $D^{1/3}x$, where D is defined by equation (24) and $x = r/a$.

as the degree of its amorphousness and the concentration of lattice defects and impurities.

7 DESORPTION PROBABILITY OF MOLECULES NEAR THE REACTION SITE

Reactions of molecules induces desorption of molecules pre-adsorbed on the site near the reaction site. The desorption probability given by equation (9) is calculated to be

$$P(r) = \frac{\nu a^2}{6\chi} x^2 \Phi(Dx^3), \quad x \equiv \sqrt{n_s} r = \frac{r}{a} \tag{21}$$

with the use of equation (1), where

$$\phi(Dx^3) = \int_0^\infty \mathrm{d}\tau \, \exp\left[-Dx^3\phi(\tau)\right] \tag{22}$$

with

$$\phi(\tau) = \tau^{3/2} \exp\left[\frac{3}{2}\left(\frac{1}{\tau} - 1\right)\right] \tag{23}$$

and

$$D = 6.79 \frac{E_\mathrm{d}}{Q} \frac{\rho c_\mathrm{p} a^3}{k}. \tag{24}$$

The numerical coefficient in D results from $4(\pi e/6)^{3/2} = 6.79$. The ratio of the desorption probabilities at distance r to $r = 0$ is calculated with the use of equation (10) to be

$$\frac{P(r)}{P(0)} = 0.408 y^{2/3} \Phi(y), \tag{25}$$

where the numerical coefficient equals $3/[2e\Gamma(2/3)]$ and

$$y = Dx^3 = D\left(\frac{r}{a}\right)^3. \tag{26}$$

Fig. 8 shows $P(r)/P(0)$ as a function of $D^{1/3}x$, i.e. the distance $x = r/a$ from the reaction site scaled by $D^{1/3}$, indicating that desorption occurs mainly in the region of $D^{1/3}x < 1$.

For numerical evaluation of $P(r)$, it is practical to use the expression of $P(0)$ given by equation (14). Then, the probability of induced desorption of a molecule adsorbed at distance r from the reaction site is expressed by

$$P_i(r) = P_0 f_i \frac{P(r)}{P(0)}, \tag{27}$$

where $P(r)/P(0)$ is given by equation (25) and is depicted in Fig. 8. We can use the values of P_0 estimated in Section 4, while the f_i values can be calculated from equation (14) by specifying the molecular species, reaction, and substrate.

As an illustrative example, let us estimate the desorption probability of pre-adsorbed CO from the site $r = a$ on H_2O ice substrate induced by H_2 formation at $r = 0$ (Duley & Williams 1993). The range of the P_0 values for H_2O ice substrate has been obtained in Section 4.2. We tentatively take a mean value of $P_0 = 0.43$. The f_i value is calculated to be $f_i = 0.49$ by adopting $Q_i = 4.5$ eV for H_2 formation (Roberts et al. 2007), $\mu_i = 28$ for a CO molecule, and $E_\mathrm{des} = 1300$ K for CO on H_2O ice (Minissale et al. 2016). The value D is estimated to be $D = 1.5$ with using the values of Q and E_d given above and $\rho c_\mathrm{p} a^3 = 9k$ for H_2O-ice substrate. In consequence, we obtain $P(a)/P(0) = 0.038$ and $P(a) \simeq 0.008$ from equation (27). $P(r)/P(0)$ increases considerably with decreasing D for $D^{1/3}x \lesssim 1.5$ as is seen in Fig. 8. If we take $D = 1$ in view of the uncertainty in the estimate of the D value, we obtain $P(a)/P(0) = 0.37$ and $P(a) \simeq 0.2$ for $P_0 = 0.43$. Appreciable desorption of a pre-adsorbed molecule from the adjacent site can occur for a combination of a reaction and a substrate having small D.

8 CONCLUDING REMARKS

We have proposed a new mechanism of desorption by impulsive spot heating due to exothermic reactions and have derived a formula of the desorption probability. The formula is based on the desorption rate of a molecule placed on a substrate of constant temperature. This theory can predict the desorption probabilities not only for one-product reactions but also for multiproduct reactions. This characteristic will be helpful to verify the theory by the experiments which involve complex reaction networks including multiproduct reactions. The other characteristic is the absence of parameters that are physically ambiguous such as a_s in Garrod et al. (2007) and the effective mass of the substrate in Minissale et al. (2016). For comparison of the theoretical and measured desorption probabilities, we have developed a practical method. This method has also been applied to the theories of Garrod et al. (2007) and Minissale et al. (2016). It has been shown that the three theories reproduce the experimental results with similar precision, although systematic experimental data giving definite desorption probability are insufficient at present. The experiments with characterization of the substrate properties, in particular, the thermal diffusivity, are encouraged to make further comparison of the theories with the experiments. It must be pointed out at the same time that this theory can also constrain the substrate properties with the use of equation (20) since the increase in the number of reactions on the same substrate narrows the range of the P_0 values, i.e. the substrate properties.

ACKNOWLEDGEMENTS

The authors thank Prof. Y. Aikawa and Prof. H. Nomura for fruitful discussion. They thank also Prof. E. F. van Dishoeck for valuable suggestions. They also thank an anonymous reviewer for constructive suggestions, which improved the original manuscript appreciably. HM acknowledges financial support by a grant-in-aid from the Ministry of Education, Culture, Sports, Science, and Technologies of Japan (25108004). OMS acknowledges NASA SMD, Astrophysics and Planetary Science Divisions for their support through the TWSC programme.

REFERENCES

Cazaux S., Minissale M., Dulieu F., Hocuk S., 2016, A&A, 585, A55

Chronological Scientific Tables, 2010, National Astronomical Observatory Japan. Maruzen Publishing, Tokyo, Japan

Chuang K.-J., Fedoseev G., Qasim D., Ioppolo S., van Dishoeck E. F., Linnartz H., 2018, ApJ, 853, 102

Cuppen H. M., Walsh C., Lamberts T., Semenov D., Garrod R. T., Pentead E. M., Ioppolo S., 2017, Space Sci. Rev., 212, 1

Duley W. W., Williams D. A., 1993, MNRAS, 260, 37

Dulieu F., Congiu E., Noble J., Chaabouni H., Moudens A., Marco Minissale M., Cazaux S., 2013, Nature Sci. Rep., 3, 1338

Garrod R. T., Wakelam V., Herbst E., 2007, A&A, 467, 1103

Hasegawa A. I., Herbst E., 1993, MNRAS, 263, 589

Hayes W. W., Oh J., Kondo T., 2012, J. Phys. Condens. Matter, 24, 104010

Ivlev A. V., R'ocker T. B., Vasyunin A., Caselli P., 2015, ApJ, 805, 59

King D. A., 1975, Surf. Sci., 47, 384

Kittel C., 1986, Introduction to Solid State Physics, 6thedn. John Wiley & Sons, New York

Landau L. D., Lifshitz E. M., 1959, Fluid Mechanics, third revised English edition. Pergamon Press, Oxford, UK

Lèger A., Jura M., Omont A., 1985, A&A, 144, 174

Minissale M., Dulieu F., Cazaux S., Hocuk S., 2016, A&A, 585, A24

Miura H., Yamamoto T., Nomura H., Nakamoto T., Tanaka K. K., Tanaka H., Nagasawa M., 2017, ApJ, 839, 47

Oba Y., Tomaru T., Lamberts T., Kouchi A., Watanabe N., 2018, Nature Astron., 2, 228

Roberts J. F., Rawlings J. M. C., Viti S., Williams D. A., 2007, MNRAS, 382, 733

Shalabiea O. M., Greenberg J. M., 1994, Å, 769, 34

Shen C. J., Greenberg J. M., Schutte W. A., van Dishoeck E. F., 2004, A&A, 415, 203

Tielens A. G. G. M., 2013, Rev. Mod. Phys., 85, 1021

Tielens A. G. G. M., Allamandola L. J., 1987, Interstellar Processes. D. Reidel Publishing Company, Dordrecht, p. 397

van Dishoeck E., 2017, in Cunningham M., Millar T. J., Aikawa Y., eds, Proc. IAU Symp. 332, Astrochemistry VII - Through the Cosmos from Galaxies to Planets . Cambridge Univ. Press, Cambridge, p. 1

van Dishoeck E., Blake G. A., 1998, ARA&A, 36, 317

Vasyunin A. I., Herbst E., 2013, ApJ, 769, 34

Vasyunin A. I., Caselli P., Dulieu F., Jiménez-Serra I., 2017, ApJ, 842, 33

Williams D. A., 1993, in Millar T. J., Williams D. A., eds, Dust and Chemistry in Astronomy. IOP Publishing, Bristol, p. 143

Yamamoto S., 2017, Introduction to Astrochemistry: Chemical Evolution from Interstellar Clouds to Star and Planet Formation, Astronomy and Astrophysics Library. Springer-Verlag, Berlin

Zhernokletov D. M., Milyavskiy V. V., Khishchenko K. V., Charakhchyan A. A., Borodina T. I., Val'yano G. E., Zhuk A. Z., 2007, CP955, Shock Compression of Condensed Matter. American Institute of Physics, New York

This paper has been typeset from a TEX/LATEX file prepared by the author.